

Supporting information

Visual Demonstration and Prediction of Hofmeister Series Based on A Poly(ionic liquid)s Photonic Array

Wenyun Li,^{‡,a} Ning Gao,^{‡,a} Wanlin Zhang,^a Kai Feng,^a Kang Zhou,^a Hongwei Zhao,^a Guokang He,^a Weigang Liu,^a Guangtao Li^{a}*

a. Department of Chemistry, Key Lab of Organic Optoelectronics & Molecular Engineering,
Tsinghua University, Beijing 100084, P. R. China

* E-mail: lgt@mail.tsinghua.edu.cn

Part 1. Supplementary Figures and Tables

Part 2. Supplementary Methods and NMR spectra

Part 1. Supplementary Figures

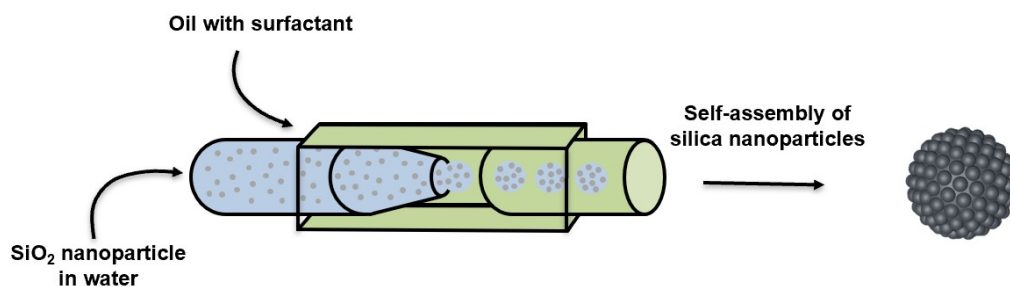


Figure S1. Schematic illustration of the preparation of the SiO₂ template microspheres by using a home-made microfluidic chip. The microfluidic chip was prepared according to our previous report (*Chem. Sci.*, **2017**,8, 6281).

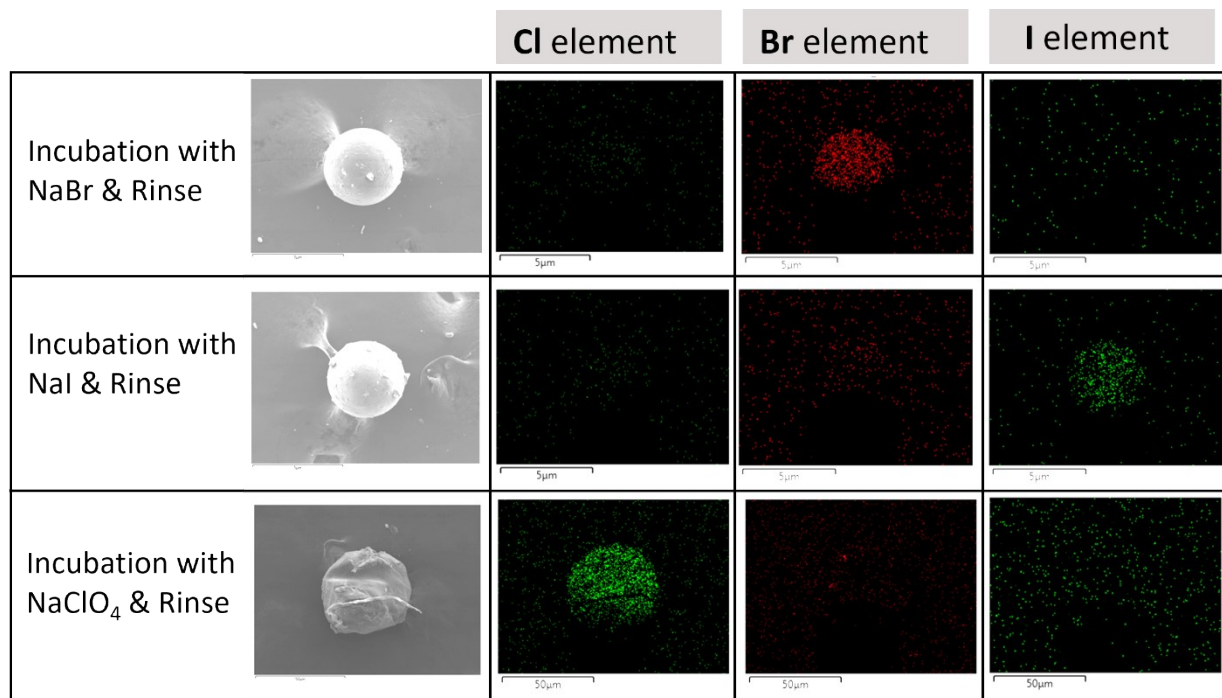


Figure S2. EDS mapping shows chloride (F), bromine (S) and iodine (I) abundant degree of PIL microspheres. These PIL microspheres were incubated with aqueous solution of different salts followed by rinsing with water for 5 times.

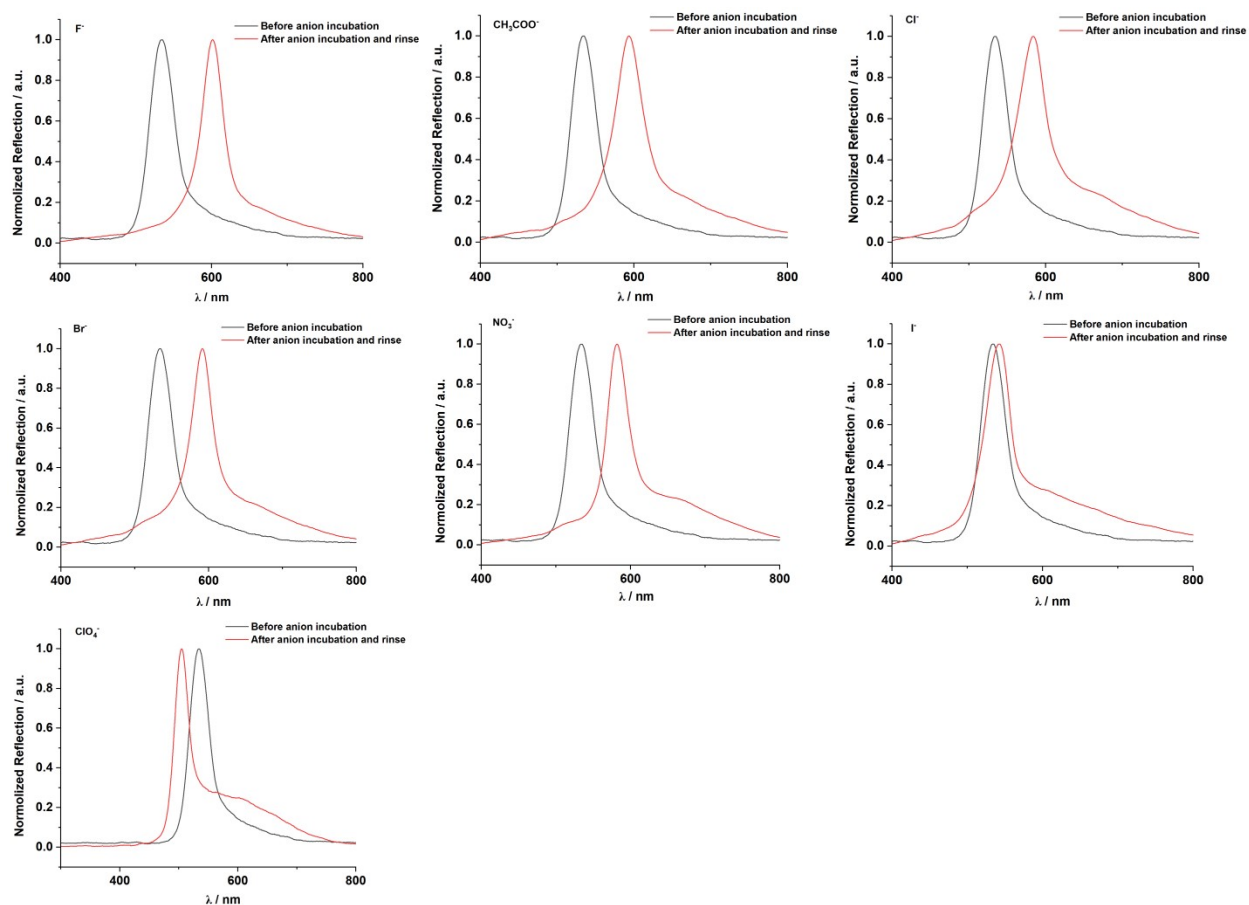


Figure S3. The peak shift of PILs microspheres before anion incubation (black line) and after anion incubation and washing five times with water (red line). Optical signals of the PIL microspheres after anion incubation and washing with water didn't restore to the initial state (before anion incubation), indicating that anion exchange occurred during the incubation process. PIL ([PY][N(CN)₂]) microspheres were employed for these control experiments.

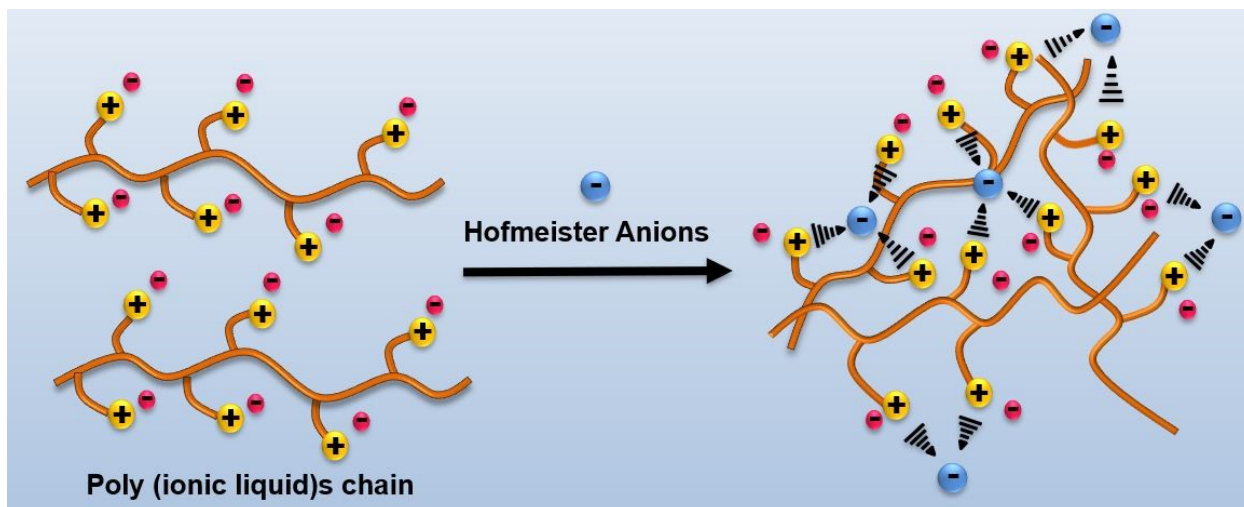


Figure S4. Schematic representation of the charge shielding effect of Hofmeister anions on overhanging cationic groups after entering the interior of PIL network.

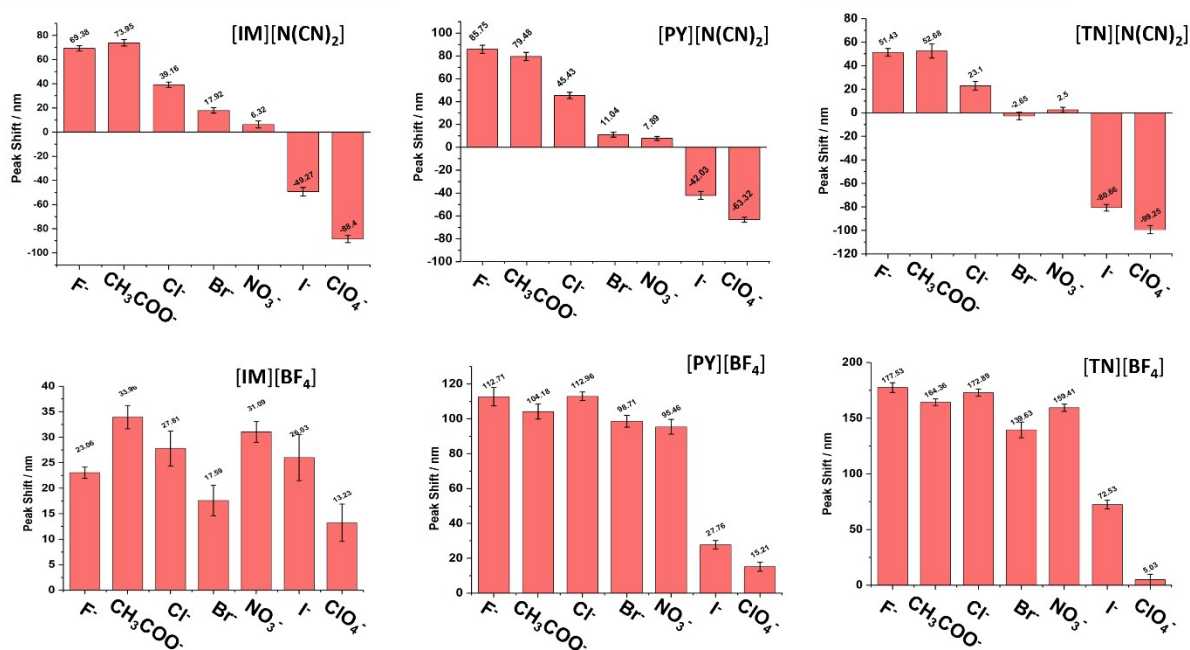


Figure S5. Plots show the reflection peak shifts of PIL microspheres as responses to different anions.

Error bars represent standard derivation (n=7).

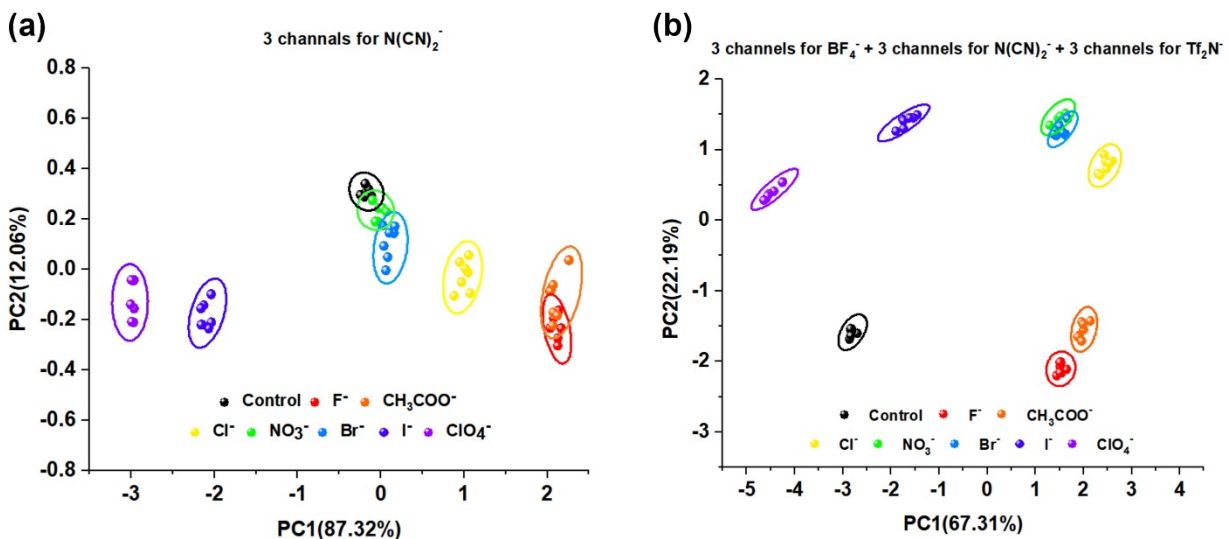


Figure S6. (a) 2D PCA score plots of 3-channels PIL photonic spheres ($[PY][N(CN)_2]$, $[IM][N(CN)_2]$ and $[TN][N(CN)_2]$) for seven Hofmeister anions. (b) 2D PCA score plots of 9-channels PIL photonic spheres ($[PY][N(CN)_2]$, $[IM][N(CN)_2]$, $[TN][N(CN)_2]$, $[PY][Tf_2N]$, $[IM][Tf_2N]$, $[TN][Tf_2N]$, $[PY][BF_4]$, $[IM][BF_4]$, $[TN][BF_4]$) for seven Hofmeister anions.

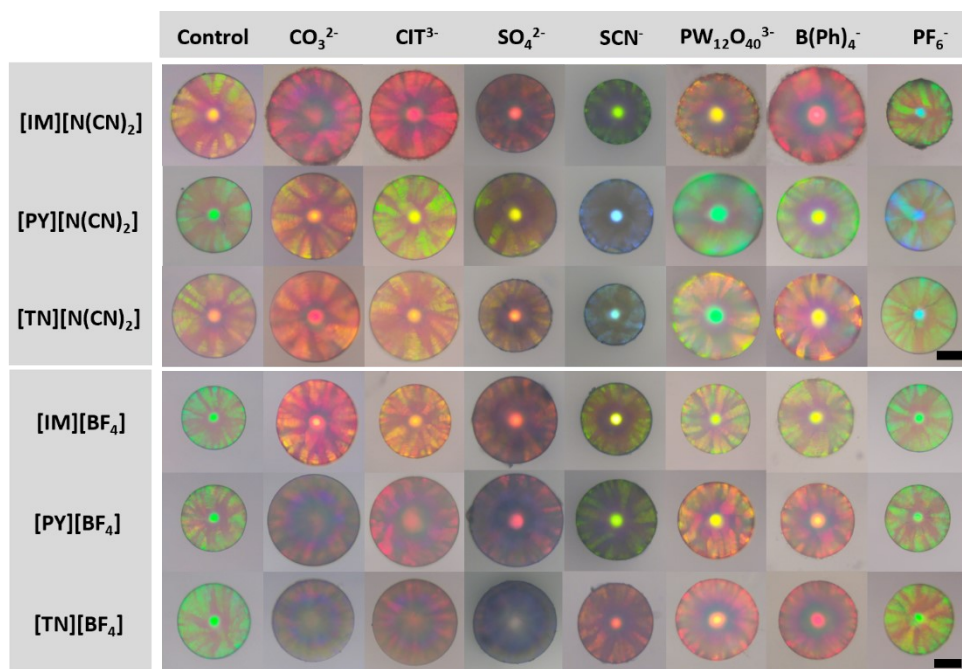


Figure S7. Optical images of the PIL microspheres consisting of different cations and anions before (labelled as “control”) and after incubation with Hofmeister anions. Scale bars are 100 μm .

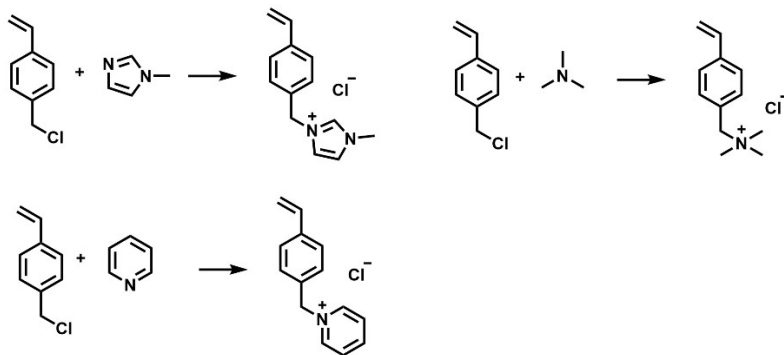


Figure S8. Synthetic routes to [IM][Cl], [TN][Cl] and [PY][Cl]. Detailed synthetic protocols were described in Supplementary Methods.

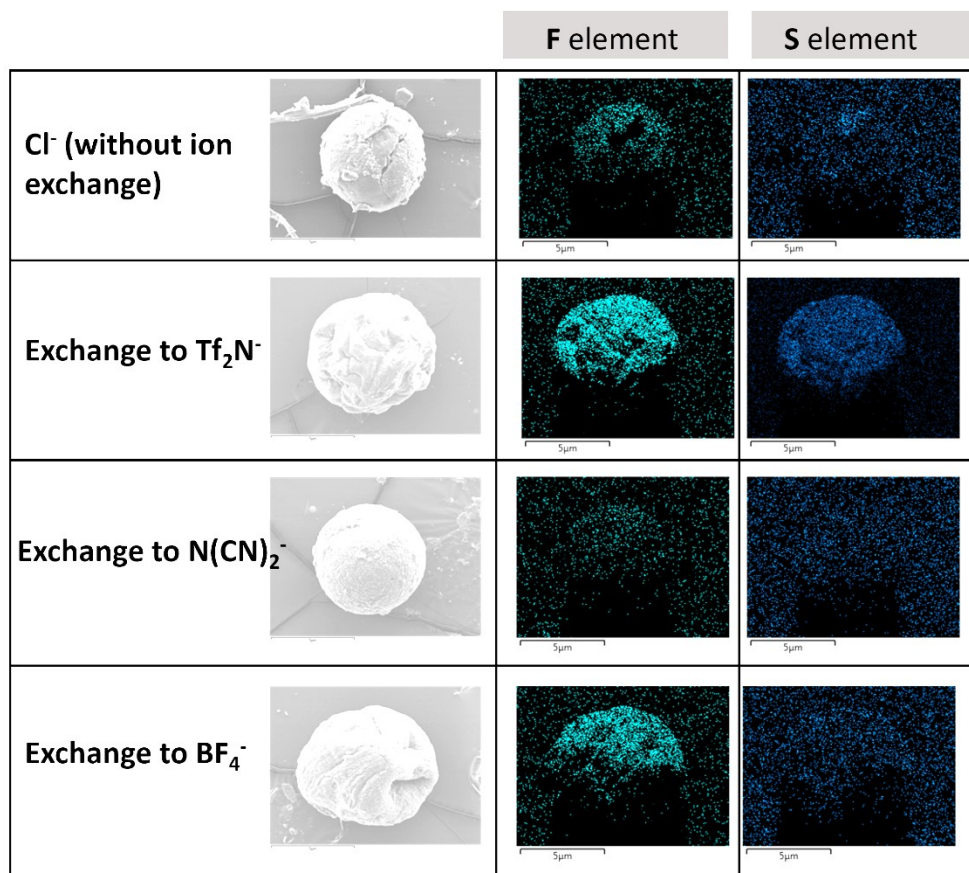


Figure S9. Element distribution scanning (EDS) mapping shows fluorine (F) and sulfur (S) abundant degree of PIL microspheres before (top row) and after (second to fourth row) anion exchange.

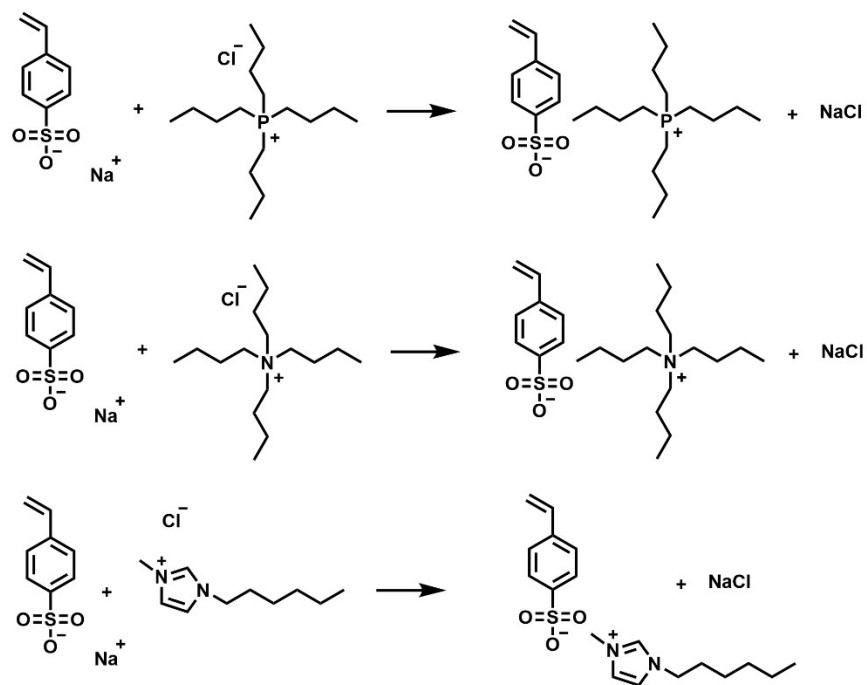


Figure S10. Synthetic routes to $[Pbu_4][SO_3]$, $[NBu_4][SO_3]$ and $[C_6mim][SO_3]$. Detailed synthetic protocols were described in Supplementary Methods.

Title	Interactions between Polyelectrolyte Brushes and Hofmeister Ions: Chaotropes versus Kosmotropes ²	Molecular Mechanism for the Interactions of Hofmeister Cations with Macromolecules in Aqueous Solution ³	Specific ion effects on the aggregation behavior of aquatic natural organic matter ⁴	Interactions of Some Hofmeister Cations with Sodium Dodecyl Sulfate in Aqueous Solution ⁵	Semihydrophobic Nanoparticle-Induced Disruption of Supported Lipid Bilayers: Specific Ion Effect ⁶
Method	Study of the interactions between the negatively charged poly(3-sulfopropyl methacrylate potassium) (PSPMA) brushes and the Hofmeister cations using a combination of quartz crystal microbalance with dissipation and spectroscopic ellipsometry.	Study of the changes of lower critical solution temperature for PNIPAM in monovalent Hofmeister chloride salt solutions. Preferential binding coefficient corresponding to a PNIPAM 20-mer chain at Hofmeister chloride salt solutions was also studied by using all-atom MD simulations.	Specific ion effects on the aggregation behavior of a reference aquatic natural organic matter (NOM), Suwannee River NOM (SRNOM), were investigated using kinetic, titration, calorimetric, and surface tension methods.	Study of the influence of some alkali metal ions on the Krafft temperature (T_K) and critical micelle concentration (CMC) of a classical ionic surfactant, sodium dodecyl sulfate (SDS), over a wide range of temperature.	Study of the specific ion effect on the interaction of semi-hydrophobic nanoparticle with zwitterionic phospholipid bilayer in aqueous media with different types of salts.
Hofmeister Cations	$NH_4^+ > K^+ > Na^+ > N(CH_3)_4^+ > Rb^+ > Cs^+$	1. $Li^+ \sim NH_4^+ < Rb^+ \sim K^+ \sim Cs^+ \sim Na^+$ 2. $Li^+ < Na^+ < Cs^+ < Ca^{2+}$	$Li^+ > Na^+ > K^+ > Rb^+ > Cs^+ > Ca^{2+}$	For T_K : $Li^+ > Na^+ > Cs^+ > K^+$ For CMC: $Cs^+ > K^+ > Na^+ > Li^+$	$Cs^+ \sim Rb^+ > Na^+ \gg N(CH_3)_4^+$
Mismatch	$Rb^+, Cs^+, N(CH_3)_4^+$	1. NH_4^+ 2. Ca^{2+}	Ca^{2+}	For T_K : Cs^+ Only 4 cations were studied.	$N(CH_3)_4^+$ Only 4 cations were studied.

Table 1. A typical Hofmeister cation series for salting-out behavior is as follows: $Mg^{2+} < Ca^{2+} < Li^+ < Na^+ < K^+ < Rb^+ < Cs^+ < NH_4^+ < N(CH_3)_4^+$.¹

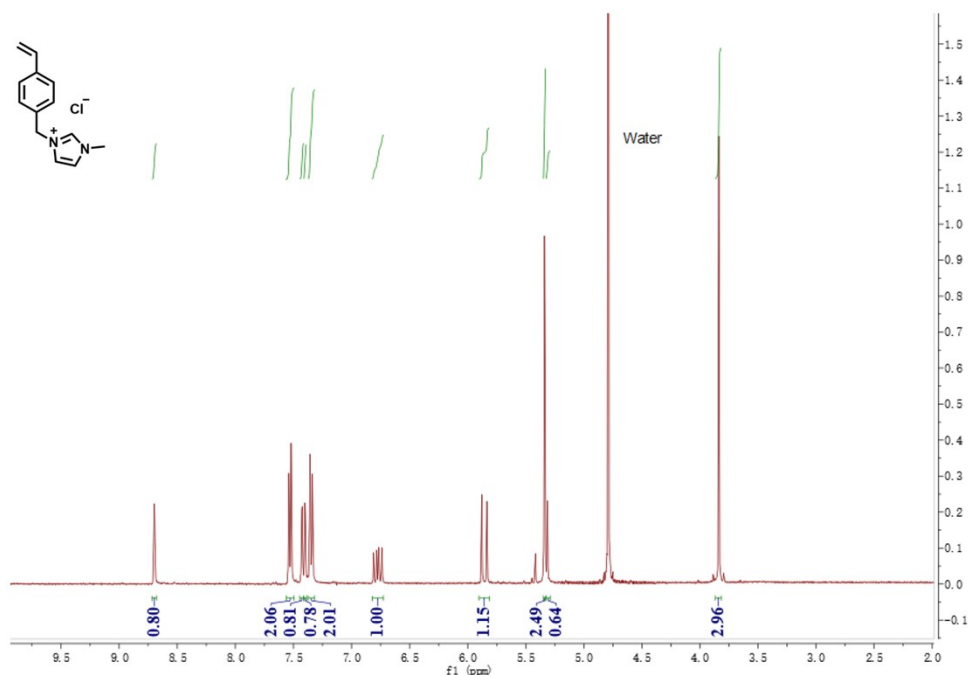
Reference :

1. J. Traube, *J. Phys. Chem.*, 1910, **14**, 452–470.
2. R. Kou, J. Zhang, T. Wang and G. Liu, *Langmuir*, 2015, **31**, 10461-10468.
3. E. E. Bruce, H. I. Okur, S. Stegmaier, C. I. Drexler, B. A. Rogers, N. F. A. van der Vegt, S. Roke and P. S. Cremer, *J. Am. Chem. Soc.*, 2020, **142**, 19094-19100.
4. F. Xu, Y. Yao, P. J. J. Alvarez, Q. Li, H. Fu, D. Yin, D. Zhu and X. Qu, *J. Colloid Interface Sci.*, 2019, **556**, 734-742.
5. K. K. Sharker, M. Nazrul Islam and S. Das, *Journal of Surfactants and Detergents*, 2018, **22**, 249-258.
6. B. Jing, R. C. Abot and Y. Zhu, *J Phys Chem B*, 2014, **118**, 13175-13182.

Part 2. Supplementary methods

Synthesis of 1-methyl-3-(4-vinylbenzyl)-1*H*-imidazol-3-ium chloride ([IM][Cl]).

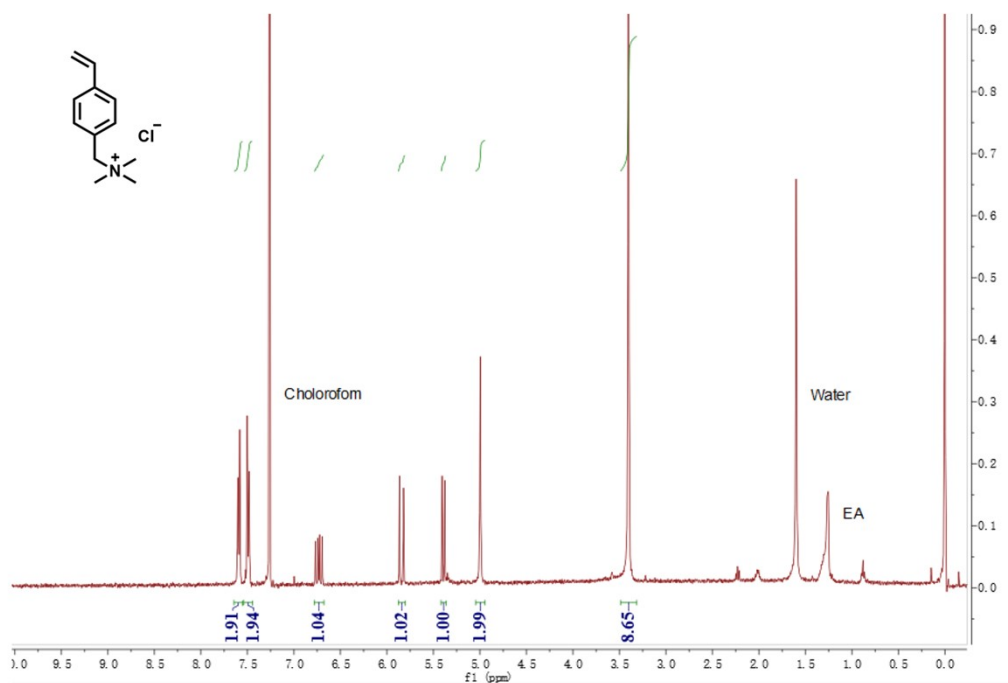
A Schlenk tube was charged with 3.50 g triethylamine (34.6 mmol, 1.00 eq), dissolved in 50 mL CHCl_3 and cooled to 0 °C. Subsequently, 7.33 mL vinylbenzyl chloride (7.92 g, 51.9 mmol, 1.50 eq) was added and the tube was heated from 0 °C to 50 °C. The mixture was stirred at 50 °C for 24 h. The mixture was extracted with water (3×40 mL), evaporated at reduced pressure to get rid of the residual organic solvents, and freeze-dried. 8.22 g of the product (94%) was obtained as colorless needles. ^1H NMR (400 MHz, D_2O) δ 8.70 (s, 1H), 7.53 (d, $J = 7.6$ Hz, 2H), 7.41 (d, $J = 9.3$ Hz, 2H), 7.35 (d, $J = 7.8$ Hz, 2H), 6.77 (dd, $J = 17.7, 11.0$ Hz, 1H), 5.86 (d, $J = 17.7$ Hz, 1H), 5.34 (s, 2H), 5.31 (s, 1H), 3.84 (s, 3H).



NMR ^1H spectra of 1-methyl-3-(4-vinylbenzyl)-1*H*-imidazol-3-ium chloride

Synthesis of *N,N,N*-trimethyl-*N*-(4-vinylbenzyl)ammonium chloride ([TN][Cl]).

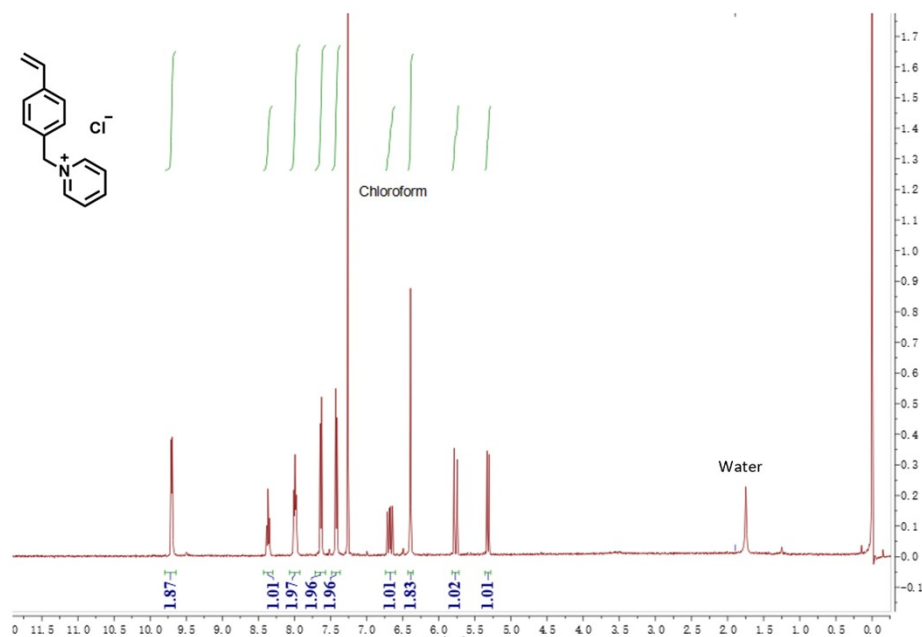
A Schlenk tube was charged with 3.50 g triethylamine (34.6 mmol, 1.00 eq), dissolved in 50 mL CHCl_3 and cooled to 0 °C. Subsequently, 7.33 mL vinylbenzyl chloride (7.92 g, 51.9 mmol, 1.50 eq) was added and the tube was heated from 0 °C to 50 °C. The mixture was stirred at 50 °C for 24 h. The mixture was extracted with water (3×40 mL), evaporated at reduced pressure to get rid of the residual organic solvents, and freeze-dried. 8.22 g of the product (94%) was obtained as colorless needles. ^1H NMR (400 MHz, CHCl_3 - d) δ 7.59 (d, $J = 8.1$ Hz, 2H), 7.49 (d, $J = 7.9$ Hz, 2H), 6.73 (dd, $J = 17.6$, 10.9 Hz, 1H), 5.84 (d, $J = 17.6$ Hz, 1H), 5.39 (d, $J = 10.9$ Hz, 1H), 4.99 (s, 2H), 3.40 (s, 9H).



NMR ^1H spectra of *N,N,N*-trimethyl-*N*-(4-vinylbenzyl)ammonium chloride

Synthesis of 1-(4-vinylbenzyl)pyridin-1-ium chloride ([PY][Cl]).

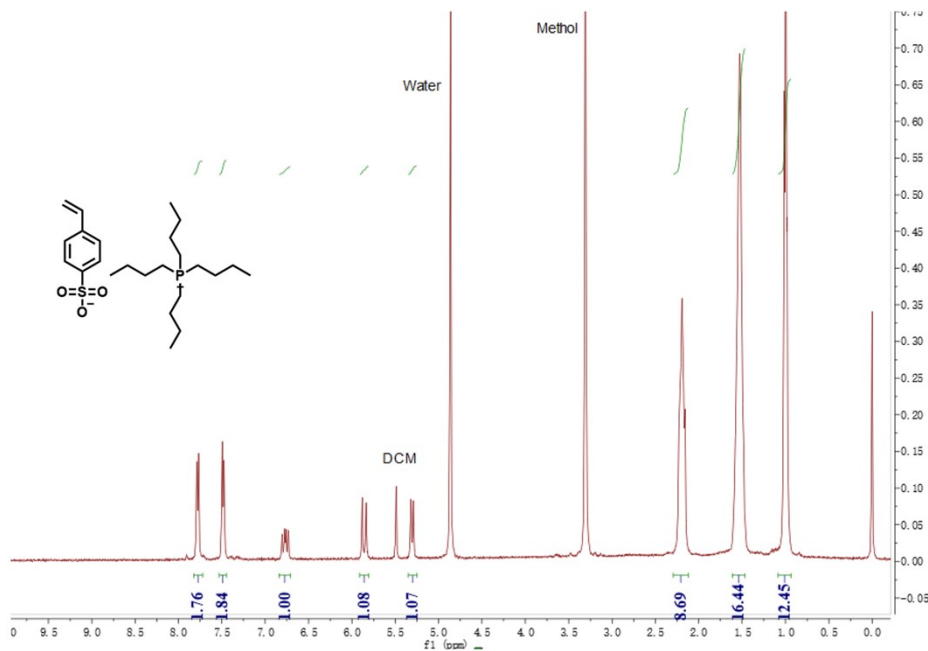
A Schlenk tube was charged with 1.24 mL pyridine (8.00 g, 52.4 mmol, 1.00 eq), dissolved in 50 mL CHCl_3 at 0 °C. 4.11 mL vinylbenzyl chloride (80%, 15.4 mmol, 1.50 eq) was added into the Schlenk tube followed by heating from 0 °C to 50 °C. The mixture was stirred at 50 °C for 24 h. The mixture was dissolved by methanol and then precipitated in 300mL ether. The filter residue was washed with ether for three times (3×300 mL). The product was then dissolved in dichloromethane and evaporated to obtain the product. 3.62 g of the product (60%) was obtained as a white powder. ^1H NMR (400 MHz, CHCl_3) δ 7.59 (d, $J = 8.1$ Hz, 2H), 7.49 (d, $J = 7.9$ Hz, 2H), 6.73 (dd, $J = 17.6, 10.9$ Hz, 1H), 5.84 (d, $J = 17.6$ Hz, 1H), 5.39 (d, $J = 10.9$ Hz, 1H), 4.99 (s, 2H), 3.40 (s, 9H).



NMR ^1H spectra of 1-(4-vinylbenzyl)pyridin-1-ium chloride

Synthesis of [Tetrabutylphosphine][4-styrenesulfonate]([PBu₄][SO₃]).

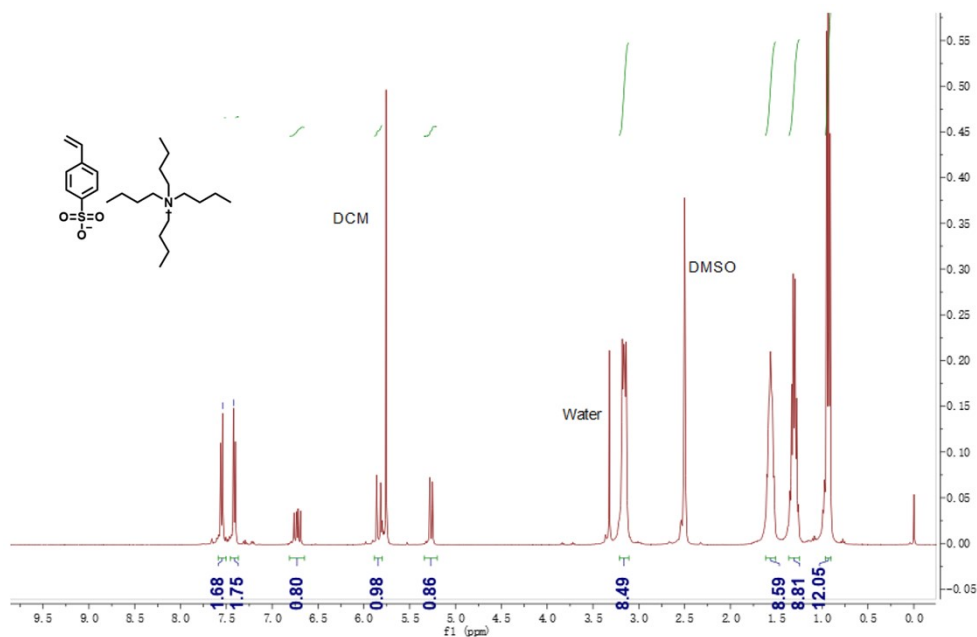
7 g of tetrabutylphosphine chloride was dissolved in 10 g water and then added by 1.2 molar equivalents of the anion salt (sodium 4-styrenesulfonate). The mixture was stirred at room temperature for 48 hours. The IL was extracted from the water phase by CH₂Cl₂. The CH₂Cl₂ was removed by a rotary evaporator and the residual liquid was dried at high vacuum for 24 hours at room temperature. The product yield was 97%. ¹H NMR (400 MHz, METHANOL-D₃) δ 7.78 (d, *J* = 7.4 Hz, 2H), 7.48 (d, *J* = 7.5 Hz, 2H), 6.77 (dd, *J* = 17.5, 11.2 Hz, 1H), 5.86 (d, *J* = 17.7 Hz, 1H), 5.31 (d, *J* = 10.9 Hz, 1H), 2.18 (d, *J* = 14.9 Hz, 9H), 1.53 (s, 16H), 1.00 (t, *J* = 6.4 Hz, 12H).



NMR ¹H plot of [Tetrabutylphosphine][4-styrenesulfonate]

Synthesis of [Tetrabutylammonium][4-styrenesulfonate] ([NBu₄][SO₃]).

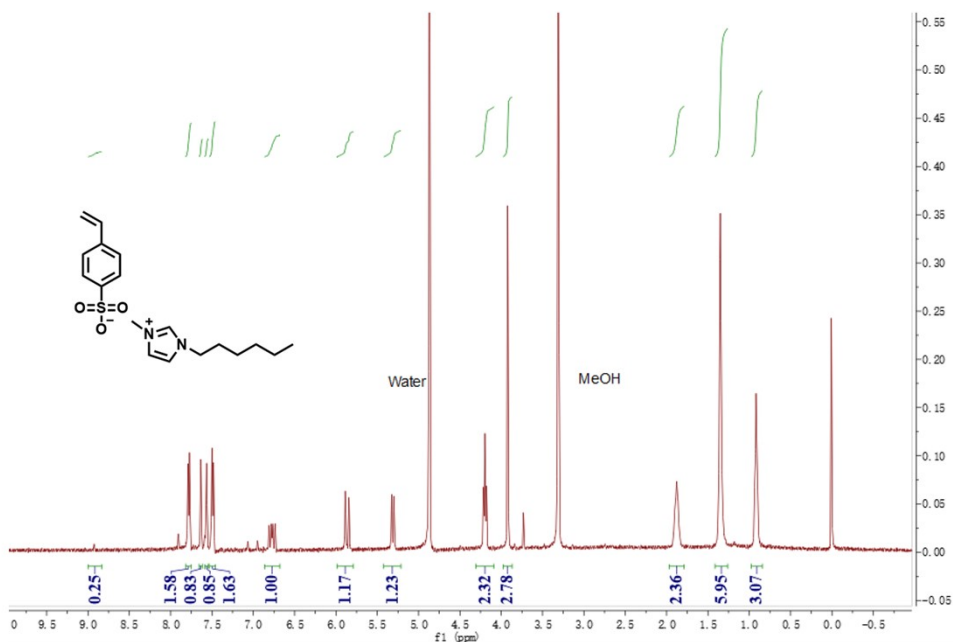
Solution of sodium 4-styrenesulfonate (1.24 g, 6.0 mmol) in H₂O (15 mL) and a solution of tetrabutylammonium chloride (1.11 g, 4.0 mmol) in CH₂Cl₂ (20 mL) were placed in separatory funnel and shaking. Organic phase was recovered and washed with brine. The solvent was evaporated and dried in vacuo to give the white powder in 90% yield. ¹H NMR (400 MHz, DMSO-d₆) δ 7.54 (s, 2H), 7.42 (s, 2H), 6.81 – 6.65 (m, 1H), 5.83 (t, *J* = 11.7 Hz, 1H), 5.28 (t, *J* = 13.6 Hz, 1H), 3.21 – 3.11 (m, 8H), 1.56 (dt, *J* = 15.5, 7.9 Hz, 8H), 1.36 – 1.25 (m, 8H), 0.93 (t, *J* = 7.3 Hz, 12H).



NMR ¹H plot of [Tetrabutylammonium][4-styrenesulfonate]

Synthesis of [1-methyl-4-hexylimidazole][4-styrenesulfonate] ([C₆mim][SO₃]).

Aqueous solution (50 mL) of 1-methyl-4-hexylimidazole chloride (10.90 g, 54.9 mmol) was added to an aqueous solution (100 mL) of sodium 4-styrenesulfonate (13.575 g, 65.04 mmol). The homogeneous mixture was stirred at room temperature overnight. The ion pair monomer product was extracted by CHCl₃. The CHCl₃ was evaporated to obtain the product. ¹H NMR (400 MHz, METHANOL-D₃) δ 8.93 (s, 1H), 7.78 (d, *J* = 6.9 Hz, 2H), 7.63 (s, 1H), 7.56 (s, 1H), 7.49 (d, *J* = 7.3 Hz, 2H), 6.77 (dd, *J* = 17.9, 11.3 Hz, 1H), 5.99 – 5.79 (m, 1H), 5.42 – 5.21 (m, 1H), 4.31 – 4.09 (m, 2H), 3.92 (d, *J* = 2.7 Hz, 3H), 1.88 (s, 2H), 1.35 (s, 6H), 0.89 (d, *J* = 26.0 Hz, 3H).



NMR ¹H plot of [1-methyl-4-hexylimidazole][4-styrenesulfonate]

PCA data analysis and Euclidean distance calculation

The implementation of the principal component analysis is performed by using the PCA function in the function package of MATLAB 2012b software. The function code is shown below:

[COEFF, SCORE, LATENT] = princomp (X)

where X represents the raw data matrix.

Euclidean distance refers to the absolute distance between two points in m-dimensional space. In 2-dimensional space, the Euclidean distance is calculated as follows :

$$ED = \sqrt{(x_2 - x_1)^2 + (y_2 - y_1)^2}$$

x_1, y_1, x_2, y_2 represent the average of the horizontal and vertical coordinates of the cluster 1 and 2.